Enhancing multiple harmonics in tapping mode atomic force microscopy by added mass with finite size

Wuweikai Xiang[1], Yanling Tian[2]*, Yue Yang[2], and Xianping Liu[2]

[1] *Institute of Systems Engineering, China Academy of Engineering Physics, Mianyang, 621999, China*

[2] *School of Engineering, University of Warwick, Coventry, CV4 7AL, UK*

E-mail: y.tian.1@warwick.ac.uk

A method to enhance the harmonics of tapping mode atomic force microscopy is proposed in this study through an attached mass with finite size. It is demonstrated that ratios between higher-order natural frequencies and the fundamental one can be tuned to be specified integers with this method. The first three eigenmodes could be excited simultaneously, defining a highly-sensitive multi-harmonic cantilever, which can be utilized to resolve the sample properties effectively. The established theoretical model is validated by finite element analysis. This method can also be developed for the determination of mass, position and geometry of micro-particle in mass sensing application.

Tapping mode atomic force microscopy (AFM) is one of the most extensively used scanning probe method for material characterization and measurement in nanoscale.[1-4] The intermittent contact between the tip and the sample surface substantially reduces the lateral force, and explains its ability to image soft materials, such as DNA, cells or polymers.[5-6] The decay length of the interaction force is, however, less than the cantilever oscillation amplitude, leading to highly nonlinear characteristics in the dynamics.[7-8] The nonlinearity could introduce higher harmonic components in the cantilever's motion, which are integer multiple of the excitation frequency. The harmonics contain important information on the sample properties. They thus allow time-resolved forces to be obtained, and make it possible for the extraction of the sample properties in microsecond.[9-12] It has been proved that the higher harmonics can be utilized effectively for both material characterization and surface imaging.[13-15] Information that is usually not resolved in the conventional method can be obtained with the multi-frequency AFM. [16-18]

Higher eigenmodes of the cantilever may be excited by the higher harmonic components as effective external forces, whenever they are close to the frequencies of the eigenmodes.[19-20] However, a higher harmonic component barely coincides with one of the natural frequencies of the cantilever. It is therefore several orders smaller than the fundamental one and may fall below the measurement noise brought by the electronics.[1] To enhance the harmonics, efforts have been made to either improve the signal to noise ratio of the tapping mode AFM or to develop specific approaches for experimental purposes, such as harmonic cantilever, bimodal excitation or band excitation.[21-23] A simple way for the enhancement of higher eigenmodes is the utilization of two driving forces vibrating at the frequencies tuned to match the first two flexural eigenfrequencies of the cantilever.[22] Besides, the multi-harmonic cantilever provides a straightforward method to enhance the higher harmonics with the simultaneous excitation of several eigenmodes, in which the modification of the shape and geometry of the cantilever could define multi-harmonic AFMs.[24-28] With the width as a variable, Cai et al. designed and optimized a variable-width harmonic probe.[26] Accordingly the natural frequencies of the cantilever could be relocated and coincide with the higher harmonics. Li et al. tuned the natural frequencies of the cantilever through the attachment of a concentrated mass, in which the second and third eigenfrequencies are integer multiples of the fundamental eigenfrequency.[27] It is an effective method from a practical standpoint. Results, however, indicate that the mass of the particle is large compared with the cantilever. The geometry and the volume of the particle thus cannot be ignored.[29-30]

In this letter, a straightforward method to construct a harmonic cantilever in tapping mode atomic force microscopy is proposed, in which an attached mass with finite size is considered to tune the resonance characteristics of the cantilever. With the consideration of the geometry and volume of the added mass, the rotational inertia and eccentricity along with its mass and position are incorporated as tuning parameters. The purpose is to relocate the natural frequencies of the cantilever to the harmonics which are integer multiples of its fundamental frequency. With the enhanced harmonics, the first three eigenmodes of the cantilever can be excited simultaneously, and thus the sensitivity of the tapping mode AFM to material properties could be improved, which enables qualitative extraction of sample property while being fast surface imaging.

An added mass of arbitrary geometry is attached to the cantilever at the location $x = l$, as depicted in Fig.1 (a). Except for the mass property (m), the rotational inertia (J) and vertical eccentricity (e) are introduced as geometric characteristics of the added particle, which contribute to the resonance of the beam. The eccentricity is defined as the distance between the mass center of the particle and the neutral axis of the cantilever. The cantilever has a uniform cross section of thickness h and width b, mass M, length L and flexural rigidity EI. Considering small deflection, the Euler-Bernouli equation is used to describe the motion of the cantilever in the sub-domains respect to the left and right side of the attached mass as[27-32)]

$$EI\frac{\partial^4 \overline{w}(\xi,t)}{\partial \xi^4} + ML^3\frac{\partial^2 \overline{w}(\xi,t)}{\partial t^2} = 0,\ 0 < \xi < \xi_l \quad \text{and} \quad \xi_l < \xi < 1 \tag{1}$$

where $\overline{w}(\xi,t)$ is the dimensionless flexural displacement of the cantilever obtained by normalizing the transverse displacement with respect to the length of the beam. $\xi = x/L$ is the dimensionless coordinate, and the parameter $\xi_l = l/L$ indicates the location of the particle attached. Assuming $\overline{w}(\xi,t) = A\varphi(\xi)e^{i\omega t}$ and including the inertial property of the particle as part of the boundary conditions, it results in a boundary value problem

$$\begin{cases} \frac{\partial^4 \Phi_1(\xi)}{\partial \xi^4} - \frac{ML^3\omega^2}{EI}\Phi_1(\xi) = 0, & 0 < \xi < \xi_l \\ \frac{\partial^4 \Phi_2(\xi)}{\partial \xi^4} - \frac{ML^3\omega^2}{EI}\Phi_2(\xi) = 0, & \xi_l < \xi < 1 \end{cases} \tag{2}$$

with the following boundary conditions

$$\Phi_1(0) = 0, \Phi_1'(0) = 0, \Phi_2''(1) = 0, \Phi_2'''(1) = 0$$
$$\Phi_1(\xi_l) - \Phi_2(\xi_l) = 0, \Phi_1'(\xi_l) - \Phi_2'(\xi_l) = 0,$$

$$\Phi_2''(\xi_l) - \Phi_1''(\xi_l) = -\alpha\lambda^4\bar{e}^2\Phi_1'(\xi_l),$$
$$\Phi_2'''(\xi_l) - \Phi_1'''(\xi_l) = \alpha\lambda^4\Phi_1(\xi_l), \tag{3}$$

where $\lambda^4 = ML^3\omega^2/EI$, $\alpha = m/M$, $\bar{e}^2 = (e^2 + J/m)/L^2$, ω is the angular frequency and the prime denotes differential with respect to ξ. Note that the dimensionless parameter α indicates the particle mass normalized by the beam mass, and $\bar{e}$ is the effective eccentricity which is the eccentricity and radius of gyration normalized by the beam length, representing the influences of the mass and geometric properties of the added mass with arbitrary geometry on the resonance characteristics of the cantilever. The frequency equation then can be obtained as $\det[\mathbf{D}(\alpha, \xi_l, \bar{e}, \lambda)] = 0$.

The determinant is expressed as

$$\begin{vmatrix} 1 & 0 & 1 & 0 & 0 & 0 & 0 & 0 \\ 0 & 1 & 0 & 1 & 0 & 0 & 0 & 0 \\ c_l & s_l & ch_l & sh_l & -c_l & -s_l & -ch_l & -sh_l \\ -s_l & c_l & sh_l & ch_l & s_l & -c_l & -sh_l & -ch_l \\ c_l - \alpha\bar{e}^2\lambda^3 s_l & s_l + \alpha\bar{e}^2\lambda^3 c_l & -ch_l + \alpha\bar{e}^2\lambda^3 sh_l & -sh_l + \alpha\bar{e}^2\lambda^3 ch_l & -c_l & -s_l & ch_l & sh_l \\ \alpha\lambda c_l + s_l & \alpha\lambda s_l - c_l & \alpha\lambda ch_l + sh_l & \alpha\lambda sh_l + ch_l & -s_l & c_l & -sh_l & -ch_l \\ 0 & 0 & 0 & 0 & -c & -s & ch & sh \\ 0 & 0 & 0 & 0 & s & -c & sh & ch \end{vmatrix} = 0 \tag{4}$$

where the following notations are introduced

$$s_l = sin\lambda\xi_l,\ c_l = \cos\lambda\xi_l,\ sh_l = sinh\lambda\xi_l,\ ch_l = \cosh\lambda\xi_l,$$
$$s = sin\lambda \quad , \quad c = \cos\lambda \quad , \quad sh = sinh\lambda \quad , \quad ch = \cosh\lambda$$

(5)

Provided the consecutive roots of the frequency equation are denoted as $\lambda_i (i = 1,2, \ldots)$ for given α, ξ_l and $\bar{e}$, the eigenfrequencies corresponding to the eigenmodes could be calculated as $\omega_i = \lambda_i^2\sqrt{EI/ML^3}$ which yields the ratio between a higher-order natural frequency (ω_i) and the fundamental one (ω_1) as $n_{i1} = \omega_i/\omega_1 = (\lambda_i/\lambda_1)^2$. Note that the ratio is totally determined by three dimensionless parameters $(\alpha, \xi_l, \bar{e})$, corresponding to the mass, location and effective eccentricity of the attached mass respectively. When the ratio n_{i1} is an integer, it indicates the eigenfrequency corresponding to a certain higher-order eigenmode coincides with the n_{i1}-th harmonic signal, which is also n_{i1}-multiple of the fundamental natural frequency. By tuning the mass, location and effective eccentricity of the attached mass $(\alpha, \xi_l, \bar{e})$ to certain optimal values, the frequency response of the cantilever corresponding to the first three eigenmodes could exhibit peak characteristics at integer multiples of the fundamental eigenfrequency. The first three eigenmodes can be excited simultaneously, and the harmonics are enhanced, providing highly-sensitive information to access the interaction force between the tip and the sample, which may help to analyze the sample property quantitatively.

In fact, the mass and effective eccentricity of the added particle with finite size are rarely independent quantities. The dependence of the mass on the effective eccentricity can simplify the selection of the optimal values of the dimensionless parameters $(\alpha, \xi_l, \bar{e})$ for regular geometry. For example, considering a solid spherical particle of radius r, dependence of the normalized mass and effective eccentricity on normalized radius ($\gamma = r/L$) is given as $\alpha = (4\pi/3)(\rho_{mass}/\rho_{beam})(\gamma^3 L^2/bh)$ and $\bar{e}^2 = (\gamma + h/2L)^2 + 2\gamma^2/5$.

The mass and effective eccentricity of a solid spherical particle could be represented by its radius once the geometry and material of the cantilever are determined. In this case, the resonance peak of the a higher-order eigenmode of a cantilever can be altered to locate at an integer multiple of the fundamental eigenfrequency through the tuning of the simplified two dimensionless parameters (ξ_l, γ), namely the location of the added mass and its radius shown in Fig.1 (b). The ratio between the second/third natural frequency and the fundamental frequency is integer at specific values of (ξ_l, γ), which is annotated on the line in Fig.2. When the normalized radius of the solid spherical particle varies from 0 to 0.05, the second natural frequency matches the 5th-9th harmonics, and the third natural frequency matches the 13th-23th harmonics. It provides a collection of (ξ_l, γ) as design parameters to change the higher-order natural frequency to coincide with the harmonic of interest.

When the intersections the specific values of (ξ_l, γ) in Fig 2 (a) and Fig 2 (b) are used, it defines a multiple harmonic cantilever, implying that the first three eigenmodes can be excited simultaneously by the harmonic signals. There are 20 combinations between the location and the radius of the particle in total. For example, when $(\xi_l, \gamma) = (0.2732, 0.0447)$, the second and third eigenfrequencies coincide with the 5th and 13th harmonics respectively. Note that when the normalized radius of the particle ($\gamma = r/L$) is less than 0.02, the second natural frequency could not match any harmonic, which is the same while $\gamma < 0.01$ in the third natural frequency. Consider a common cantilever in tapping mode AFM with the length and thickness of 200μm and 5μm, respectively. The diameter of the added particle should be no less than 8μm to define a multiple harmonic cantilever, which is larger than the thickness of the cantilever. It demonstrates that the geometry of the added mass plays a significant role in the tuning of the vibration characteristics of a micro-cantilever used in tapping mode AFM.

Typical values of the location and radius of the added particle for the design of a multiple harmonic cantilever are listed in Table 1. Results predicted by the finite element method are also displayed. Finite element analysis results are in good agreement with the theoretical ones. The relative error is below 1%, indicating the feasibility of the proposed method. The enhancement of the harmonics in the dynamics of the cantilever helps to estimate the interaction forces which are directly associated with the sample properties. Besides, in the tuning process, given geometry properties of the particle as well as its mass and position determines the frequency spectra of the cantilever. The inverting process could, therefore, be developed to convert the frequency data to the information of the particle with back-calculation algorithms analogous to recent methods related to the mass detection.

In summary, a tuning method for the enhancement of higher-order harmonics in tapping mode AFM is proposed with the attachment of a finite size mass. Tuning parameters include the mass and position of the attached mass, as well as its rotational inertial and eccentricity to the beam axis with the consideration of its geometry and volume. A collection of tuning parameters can be determined to make the higher-order natural frequency coincide with the harmonic of interest. It could further define multi-harmonic cantilevers, in which the eigenfrequencies corresponding to the second and third flexural eigenmodes are altered to locate at integer multiples of the fundamental one. The first three eigenmodes of the cantilever could be excited simultaneously by the harmonics generated by the tip-sample interaction forces, enhancing the harmonic signals and providing the ability of surface property extraction without compromising topology acquisition speed in tapping mode AFM. Resonance characteristics are also calculated using the finite element method with the typical values of the location and radius of an added spherical particle obtained from the proposed model. Results show excellent agreement, which verifies the effectiveness of the established model. This method could further be extended to determine the position, mass and geometry of a particle of finite size attached to a beam in mass sensing of nano-mechanical applications with the development of back-calculation algorithms.

Acknowledgments

This research is supported by EU H2020 MSCA RISE MNR4SCell (no. 734174).

References

1) R. Garcia, and E. T. Herruzo, Nat. Nanotechnol. **7**, 217 (2012).
2) S. Sasaki, Y. Kobayashi, L. Zheng, K. Suenaga, Y. Maniwa, Y. Miyauchi, and Y. Miyata, Appl. Phys. Express **9**(7), 071201 (2016).
3) Y. F. Dufrêne, T. Ando, R. Garcia, D. Alsteens, D. Martinez-Martin, A. Engel, C. Gerber, and D. J. Müller, Nat. Nanotechnol. **12**, 295 (2017).
4) J. He, Y. Zhong, Y. Zhou, X. Guo, Y. Huang, J. Liu, M. Feng, Q. Sun, M. Ikeda, and H. Yang, Appl. Phys. Express **12**(5), 055507 (2019).
5) J. L. Garrett, L. J. Krayer, K. J. Palm, and J. N. Munday, Appl. Phys. Lett. **111**, 043105 (2017).
6) S. Benaglia, V. G. Gisbert, A. P. Perrino, C. A. Amo, and R. Garcia, Nat. Protoc. **13**, 2890 (2018).
7) A. Keyvani, H. Sadeghian, H. Goosen, and F. V. Keulen, Appl. Phys. Lett. **112**, 163104 (2018).
8) E. Rull Trinidad, T. W. Gribnau, P. Belardinelli, U. Staufer, and F. Alijani, Appl. Phys. Lett. **111**, 123105 (2017).
9) J. R. Lozano, and R.Garcia, Phys. Rev. Lett. **100**, 076102 (2008).
10) M. Stark, R. W. Stark, W. M. Heckl, and R. Guckenberger, Proc. Natl. Acad. Sci. U.S.A. **99**, 8473 (2002).
11) S. Zhang, J. Qian, Y. Li, Y. Zhang, and Z. Wang, Microsc. Microanal. **24**, 256 (2018).
12) Z. Wang, J. Qian, Y. Li, Y. Zhang, Z. Song, Z. Dou, and R. Lin, Micron **118**, 58 (2019).
13) M. Balantekin, and A. Atalar, Appl. Phys. Lett. **87**, 243513 (2005).
14) Y. M. Efremov, A. X. Cartagena-Rivera, A. I. M. Athamneh, D. M. Suter, and A. Raman, Nat. Protoc. **13**, 2200 (2018).
15) F. Gramazio, M. Lorenzoni, F. Pe´rez-Murano, L. Evangelio, and J. Fraxedas, Ultramicroscopy **187**, 20 (2018).
16) R. Takahashi, and T. Okajima, Appl. Phys. Lett. **107**, 173702 (2015).
17) S. Y. Kim, D. Khanal, B. Kalionis, and W. Chrzanowski, Nat. Protoc. **14**, 576 (2019).
18) S. Santos, C. Lai, T. Olukan, and M. Chiesa, Nanoscale **9**, 5038 (2017).
19) R. W. Stark, G. Schitter, M. Stark, R. Guckenberger, and A. Stemmer, Phys. Rev. B **69**,

085412 (2004).

20) T. R. Rodrıguez, and R. García, Appl. Phys. Lett. **80**, 1646 (2002).
21) A. Keyvani, H. Sadeghian, M. S. Tamer, J. F. L. Goosen, and F. V. Keulen, J. Appl. Phys. **121**, 244505 (2017).
22) T. R. Rodrıguez, and R. García, Appl. Phys. Lett. **84**, 449 (2004).
23) S. Jesse, S. V. Kalinin, R. Proksch, A. P. Baddorf, and B. J. Rodriguez, Nanotechnology, **18**, 435503 (2007).
24) G. Göring, P. I. Dietrich, M. Blaicher, S. Sharma, J. G. Korvink, T. Schimmel, C. Koos, and H. Hölscher, Appl. Phys. Lett. **109**, 063101 (2016).
25) M. Loganathan, D. A. Bristow, Rev. Sci. Instrum. **85**, 043703 (2014).
26) J. Cai, Q. Xia, Y. Luo, L. Zhang, and M. Y. Wang, Appl. Phys. Lett. **106**, 071901 (2015).
27) H. Li, Y. Chen, and L. Dai, Appl. Phys. Lett. **92**, 151903 (2008).
28) N. Alsharif, A. Burkatovsky, C. Lissandrello, K.M. Jones, A.E. White, and K.A. Brown, Small **14**(19), 1800162 (2018).
29) H. R. Ali-Akbari, S. Ceballes, and A. Abdelkefi, Physica E **94**, 31 (2017).
30) M. Shaat, and A. Abdelkefi, Int. J. Mech. Sci. **101**, 280 (2015).
31) S. Heinrich, and I. Dufour, Sensors, **15**, 29209 (2015).
32) C. Ma, Y. Chen, J. Chen, and J. Chu, Appl. Phys. Express **9**(11), 116601 (2016).

Figure Captions

Fig. 1. (a) An added mass (m) of arbitrary geometry is attached to a uniform cantilever at the location $x = l$ to enhance the harmonics. The geometry properties of the added mass are reflected in its rotational inertial J and eccentricity e respect to the beam axis. (b) Frequency response of the enhanced cantilever (harmonic cantilever) is compared with that of the original cantilever. The 6-th and 17-th harmonics can be significantly enhanced by the second and third eigenmodes of the harmonic cantilever. (ξ_l = 0.3826, γ = 0.0205, $\rho_{mass}/\rho_{beam} = 8$, $L^2/bh = 200$)

Fig. 2. Dependence of ratio between higher natural frequency and the fundamental natural frequency of the cantilever on location (ξ_l) and radius (γ) of a solid spherical particle: (a) $n_{21} = \omega_2/\omega_1$, (b) $n_{31} = \omega_3/\omega_1$. The projection is the intersection between the ratio surface and the planes with integer ratios, where the integer ratios are annotated on the curves. ($\rho_{mass}/\rho_{beam} = 8$, $L^2/bh = 200$)

Table I. Typical values of particle location and radius to enhance harmonics obtained by theoretical model and validated by finite element method.

ξ_l	γ	Euler-Bernouli Model		Finite Element Method				
		n_{21}	n_{31}	f_1 (MHz)	f_2 (MHz)	f_3 (MHz)	n_{21}	n_{31}
0.2733	0.0447	5	13	0.1024	0.5135	1.3331	5.01	13.01
0.1888	0.0334	6	15	0.1038	0.6195	1.5581	5.97	15.01
0.6982	0.0353	7	18	0.0825	0.5787	1.4818	7.01	17.96
0.7357	0.0439	8	20	0.0748	0.5951	1.5084	7.96	20.17

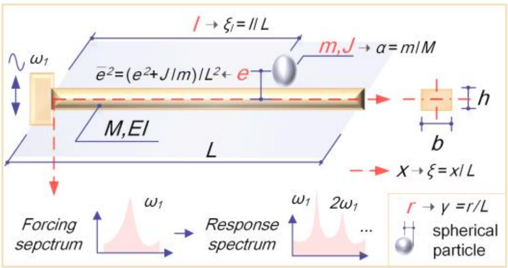

$l \to \xi_l = l/L$
$m,J \to \alpha = m/M$
$\bar{e}^2=(e^2+J/m)/L^2 \leftarrow e$
ω_1
M,EI
L
h
b
$x \to \xi = x/L$
$r \to \gamma = r/L$
Forcing sepctrum
Response spectrum
ω_1
$2\omega_1$
spherical particle

(a)

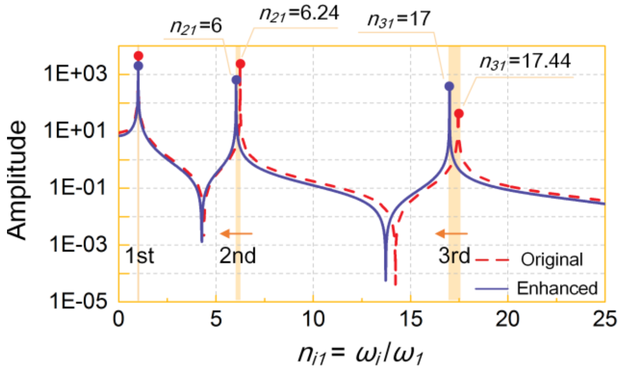

n_{21}=6
n_{21}=6.24
n_{31}=17
n_{31}=17.44
Amplitude
1E+03
1E+01
1E-01
1E-03
1E-05
1st
2nd
3rd
Original
Enhanced
0
5
10
15
20
25
$n_{i1}= \omega_i/\omega_1$

(b)

Fig.1.

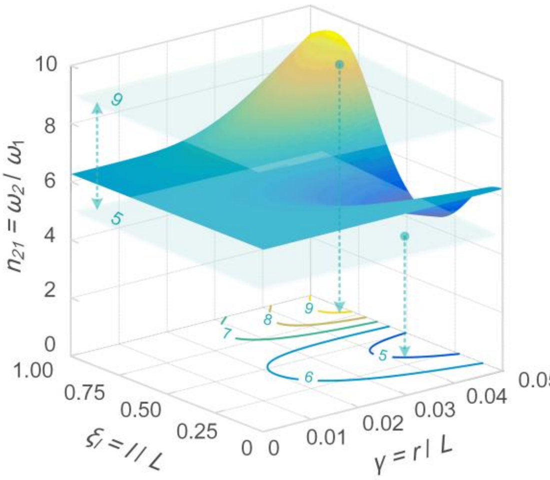

10
8
6
4
2
0
9
5
$n_{21} = \omega_2 / \omega_1$
7
8
9
7
5
6
1.00
0.75
0.50
0.25
0
0
0.01
0.02
0.03
0.04
0.05
$\xi_l = l / L$
$\gamma = r / L$

(a)

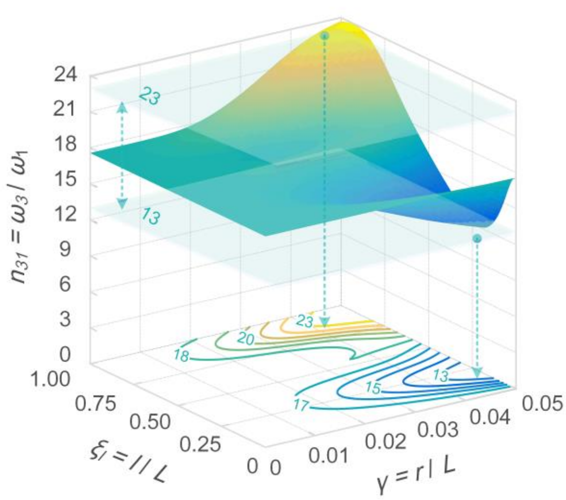

24
21
18
15
12
9
6
3
0
23
13
$n_{31} = \omega_3 / \omega_1$
20
23
18
15
13
17
1.00
0.75
0.50
0.25
0
0
0.01
0.02
0.03
0.04
0.05
$\xi_l = l / L$
$\gamma = r / L$

(b)

Fig. 2.